
Article:
Wilson, Samuel, Farren, Naomi orcid.org/0000-0002-5668-1648, Bernard, Yoann et al. (5 more authors) (2025) Influence of Vehicle Design on Near-Road Concentrations of Traffic-Related Air Pollutants. ACS ES&T Air. pp. 1089-1098. ISSN 2837-1402

https://doi.org/10.1021/acsestair.5c00059

ACS ES&T Air

pubs.acs.org/estair

Article

Influence of Vehicle Design on Near-Road Concentrations of Traffic-Related Air Pollutants

Samuel Wilson, Naomi J. Farren, Yoann Bernard, Marvin D. Shaw, Kaylin Lee, Mallery Crowe, James D. Lee, and David C. Carslaw*

Cite This: *ACS EST Air* 2025, 2, 1089–1098

Read Online

ACCESS | Metrics & More | Article Recommendations | Supporting Information

ABSTRACT: Exposure to traffic-related air pollution (TRAP) is an ongoing health concern worldwide, particularly close to roads where concentrations are the highest. Near-road exposure is influenced by factors such as vehicle exhaust emission rates, pollutant composition, and dispersion behavior. In this work we apply a recently developed technique called *plume regression* based on fast-response roadside measurements, to better understand the variables affecting near-road TRAP concentrations. Of specific interest is determining the extent to which vehicle design and physical characteristics affect roadside exposure to important pollutants such as nitrogen oxides (NO_x = NO + NO_2). We find that the position of passenger car's exhaust (tailpipe)—whether on the left or right side—results in a 40% difference in pollutant concentration contribution at the curbside. In the UK, only 20.1% of diesel passenger cars, the most significant vehicle class contributors to NO_x emissions, have their exhausts positioned on the right, the position associated with the lowest concentrations. If all diesel cars in the UK were equipped with right-positioned exhausts—the side farthest from the curb, curbside concentrations from these vehicles would be reduced by one-third. We also find evidence that electric vehicles (EVs) act to dilute the exhaust plumes of proximate fossil-fueled vehicles through vehicle-induced turbulence, reducing near-road TRAP exposure, a hitherto unrealized benefit of EVs.

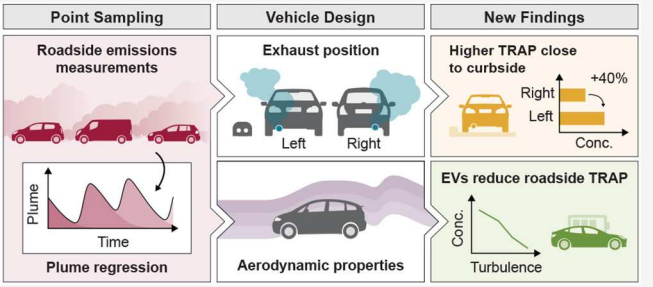

KEYWORDS: *Vehicle emissions, traffic-related air pollution, exhaust position, aerodynamic design, electric vehicles*

1. INTRODUCTION

Traffic-related air pollution (TRAP) has long been recognized as having significant impacts on human health and the wider environment.[1−3] An important way of studying TRAP is through ambient air quality measurements made close to roads. There are thousands of near-road ambient air quality measurement sites around the world that serve the primary purpose of monitoring the influence of road traffic on air pollution. Such sites typically report concentrations at an hourly resolution, which allows a comparison of measured concentrations with air quality standards and guidelines, many of which have an hourly mean averaging time.[4] Faster-response measurements of at least 1 Hz have increasingly been used for mobile measurements to map pollutant concentrations spatially, and to estimate emission intensities.[5−7] In part, this increase in the use of fast-response measurements reflects the developments in instrumentation. However, there are far fewer studies that have adopted similarly fast measurements at fixed locations.[8−10]

Reducing measurement sampling times offer the potential to develop an enhanced understanding of TRAP, which is important for developing strategies to mitigate air pollution and its health and environmental impacts, particularly in urban areas where exposure is highest.[11] As instrument averaging times approach one or a few seconds, near-road measurements can resolve individual exhaust plumes from passing vehicles, greatly enhancing the potential to gain information about emission sources. At this temporal resolution, it is possible (but challenging) to quantify emissions from individual vehicles by integrating plume concentrations and using ratios to carbon dioxide (CO_2) to derive fuel-based emission factors.[12] In related work, Farren et al. recently developed a new technique called *plume regression*, which greatly simplifies the quantification of vehicle emissions.[13] This method leverages fast-response road-side measurements of dispersing vehicle exhaust plumes, eliminating the need to identify and extract individual vehicle plumes. Additionally, Farren et al. demonstrated that such measurements can be used for concentration source apportionment, enabling the quantifica-

Received: February 28, 2025
Revised: May 12, 2025
Accepted: May 13, 2025
Published: May 21, 2025

tion of total concentration contributions by vehicle type, which is valuable new information.

High temporal resolution roadside measurements, capable of resolving individual vehicle plumes, present an opportunity to investigate the factors that control near-road TRAP concentrations. Critical data in this respect are information about the individual vehicles passing the measurement location. Automatic number/license plate recognition (ANPR/ALPR) systems enable the efficient capture of number plates for thousands of vehicles, which can then be used to query national vehicle databases. In the UK, like many other countries, these databases provide comprehensive technical information, including fuel type and emission standard as well as vehicle characteristics such as dimensions and mass. Coupling this technical information with techniques for analyzing fast-response roadside measurements allows for a deeper investigation of the relationship between vehicle design characteristics and near-road concentrations of TRAP.

Previous work, including computational studies by Plogmann et al., has demonstrated that vehicle speed and design characteristics such as exhaust position are important factors influencing exhaust plume dispersion.[14,15] In this paper, we apply the *plume regression* approach to real-world emissions measurements to better understand the vehicle-related factors that control near-road concentrations of TRAP. Of principal interest is the extent to which the physical design characteristics of vehicles affect measured concentration contributions. Specifically, we consider the exhaust (tailpipe) position and vehicle aerodynamic properties. The proximity of the exhaust to the curb likely influences the degree of plume dilution, whereas the aerodynamic properties, such as physical size, are expected to affect vehicle-induced turbulence, thereby impacting near-road dispersion and concentrations. Additionally, we explore the growing role of electric vehicles (EVs) in the fleet and their influence on near-road TRAP concentrations; particularly how EVs contribute to the dilution of exhaust plumes from fossil-fueled vehicles through vehicle-induced turbulence.

This study represents the first instance where individual vehicle measurements have been used to investigate these variables, offering a novel perspective on how vehicle design influences roadside TRAP concentration. While the focus is on measurements made in the UK, the approach and findings are applicable to urban settings globally, providing transferable insights that could improve the quantification of TRAP at the thousands of near-road ambient air quality sites that exist worldwide.

2. MATERIALS AND METHODS

2.1. Point Sampling. *2.1.1. Instrumentation.* Nitrogen oxides (NO_x = NO + NO_2) and CO_2 were measured at 1 Hz using an Airyx Iterative Cavity Enhanced Differential Optical Absorption Spectrometer (ICAD).[16] The ICAD instrument was placed on a trolley at the curbside and sampled through a 30 cm length of 1/4″ diameter perfluoroalkoxy tubing for continuous measurement of vehicle exhaust plumes. The instrument directly measures nitrogen dioxide (NO_2) in the 430−465 nm range through optical absorption, with an internal ozone-based gas phase titration system converting nitric oxide (NO) to NO_2, allowing for total NO_x and NO measurements. CO_2 is measured simultaneously via a non-dispersive infrared sensor. Further technical details are available in the literature.[17]

A custom-built device was deployed approximately 1 m upstream of the ICAD instrument to record vehicle pass times. Optical sensors within the device measure vehicle speed and acceleration, triggering a camera positioned a further 5−10 m upstream of the device to capture rear images of passing vehicles. All equipment was powered using two portable power stations with a capacity of 512 and 256 Wh. Images of the roadside measurement sites can be found in Figure S1.

2.1.2. Measurement Surveys. Point sampling (PS) surveys were conducted at three sites in York, UK: two on the University of York campus (latitude 53.947, longitude −1.047) and one in a light industrial area near a large retail park (latitude 53.987, longitude − 1.103); the locations were designated as sites A, B, and C respectively. Measurement surveys were carried out on weekdays between September and November 2023, during daylight hours and dry weather, with ambient temperatures ranging from 1.9 to 18.7 °C (12.9 °C mean).

Registration (license plate) numbers were extracted from the vehicle images using ALPR software (Rekor CarCheck Plus).[18] The registration numbers were sent to CDL Vehicle Information Services Limited to obtain vehicle technical data. CDL sources this information from the UK vehicle taxation system (DVLA) and the Society of Motor Manufacturers and Traders (SMMT) Motor Vehicle Registration Information System. The technical data includes a range of information, including, but not limited to, vehicle type, fuel type, mass, dimensions, make, model, registration date, and emission standard.

In total, 11,264 vehicle passes (7,955 unique vehicles) were recorded over 9 measurement days, with 14.7%, 23.9%, and 61.4% of measurements being made at sites A, B, and C, respectively. Technical information was obtained for 95% of the vehicle passes. A summary of the driving conditions and measured vehicle fleet composition at each site is provided in Table S1.

2.2. Analysis Methods. *2.2.1. Plume Regression.* A *plume regression* technique is used to quantify the contribution from different types of vehicle that best explains the roadside concentration time series measurements.[13] For the NO_x and CO_2 concentration time series, the increments above a local background were determined for each pollutant. While various methods can be used, a simple rolling average low percentile approach was chosen, using a time window of 100 s.[6,7,19] This window was selected to comfortably encompass the typical width of an exhaust plume of ≈20 s, while minimizing the capture of contributions from sources other than passing vehicles.

Instead of attempts to isolate individual vehicle plumes, the technique uses a statistical approach to quantify concentration contributions for different categories of all passing vehicles. An average exhaust plume profile is derived from CO_2 measurements from isolated vehicles (where there is at least a 20 s gap between vehicle passes before and after, n = 306).[13] This plume profile represents the expected average rise and fall of concentrations after a vehicle passes. As noted by Farren at al., in some situations different plume profiles could be used, e.g., for different sites or for heavy vehicles with a vertical exhaust.

The effect of the plume profile shape is considered in more detail in the Supporting Information (Figures S2 and S3). In the current work, however, similar plume profiles were observed at all three measurement sites, and one average plume profile was used for all vehicle groups. Additional site-

https://doi.org/10.1021/acsestair.5c00059
ACS EST Air 2025, 2, 1089−1098

specific analyses were conducted to confirm the suitability of this approach, with the results presented in the Supporting Information (Figures S4 and S5, Table S2).

In previous work by Farren et al., roadside concentration data were processed to provide emission factors by vehicle fuel and technology types, e.g., a Euro 5 diesel passenger car.[13] The way in which the data are disaggregated is determined at the beginning of the analysis. In the current application, the interest is not the technologies but the design characteristics of a vehicle such as the exhaust position for gasoline and diesel passenger cars. Each time a vehicle from a particular category passes (such as a gasoline vehicle with an exhaust positioned on the left-hand side), a normalized plume is added to the time series column for that category of vehicle. This process continues to cover all vehicle categories (determined by the initial disaggregation) of interest and for all passing vehicles; the same averaged normalized plume profile determined from isolated vehicle measurements was used for all vehicle categories. The main aim of the analysis is to determine the optimal amount by which the vehicle category plumes must be multiplied by to best explain the robust linear regression that relates the concentration of CO_2 or NO_x to the different vehicle category plumes.[20] The coefficients from the regression provide a direct estimate of the concentration contribution from each vehicle category. A useful benefit of the regression-based approach is that the standard errors are provided for each regression coefficient from which 95% confidence intervals can be derived.

CO_2 was used as a tracer for TRAP in the plume regression technique due to its high concentration in exhaust gases, stability under ambient conditions, direct proportionality to fuel combustion, and independence from exhaust after-treatment systems. These features make CO_2 an ideal tracer for assessing how vehicle design affects exhaust plume dispersion and subsequent roadside concentrations of TRAP, which can be assumed to disperse similarly to CO_2.[14] CO_2 exhaust gas concentrations vary for diesel and gasoline fuels based on differences in the air/fuel ratio utilized for combustion. However, the differences in absolute CO_2 emissions output are small, and discussed further in Section 3.1. NO_x and NO_2 were also analyzed to provide direct evidence of the influence of vehicle design on roadside TRAP concentrations and to provide information that could be used to derive emission factors.

2.2.2. Vehicle Design Properties Assignment. Exhaust exit positions were assigned from the vehicle images for passenger cars only, as other vehicle types rarely showed visible exhausts or did not exhibit varied placement. Of 8,643 car measurements, 44.4% were manually assigned and as either 'left', 'right', 'center', or 'split', while the 2.9% of EVs were assigned as 'none'. The assignments, based on the rear of the vehicle relative to UK traffic flow, define left as curbside, right as offside, split for exhaust exits in both positions, and center as middle placement. Examples for each assignment are shown in Figure S6.

The remaining cars were not assigned manually, due to nonvisible down-turned exhaust exits, often hidden by the rear bumper. A random forest model was used to predict exhaust positions for these vehicles as either left or right, as split or center exhausts are rarely down-turned or hidden by other design features.[21,22] This machine learning algorithm, chosen for its ability to handle categorical data, was trained on the manually assigned data (80% training and 20% validation). Predictor variables included the fuel type, Euro emission class, body type, manufacture year, number of doors, seat count, drive axle configuration, transmission type, and gear count. Features were selected to balance model robustness with the need for complete data; the model showed high classification accuracy, with an F1-score of 0.94 and Matthews correlation coefficient of 0.85. Following exhaust prediction, 95.5% of cars (8597 measurements) had assigned exhaust positions, with the remaining unknowns due to insufficient predictor variable data. Tables S3 and S4 provide detailed model performance metrics and a summary of the number of manually assigned and predicted exhaust positions. To evaluate the influence of exhaust position on near-road TRAP concentrations, vehicles were grouped by type, fuel type, and exhaust position in the plume regression analysis.

Aerodynamic drag coefficients (C_d) quantify a vehicle's air resistance, and are directly proportional to vehicle-induced turbulence (Section 2.2.3). Vehicles were assigned a C_d value based on market segment classifications derived from their dimensions. Passenger cars were grouped into eight segments (A, B, C, D, E, F, J, and S), while light goods vehicles (LGVs) formed a separate segment (V). Vehicles with missing dimension information, including heavy goods vehicles (HGVs) and buses, were classified as unknown. Estimated C_d values from the literature were then assigned to each segment.[23,24] Table S5 provides dimension classifications and C_d values for each segment.

2.2.3. Vehicle-Induced Turbulence. Vehicle-induced turbulence plays an important role in exhaust gas dispersion and directly influences roadside TRAP concentrations. Turbulent kinetic energy (TKE), measured using a sonic anemometer, has been used to evaluate the relationship between near-road TRAP and vehicle-induced turbulence.[15,25,26] In this study, we consider the power required to overcome aerodynamic drag, P_d, which is directly proportional to the TKE and reflects the energy available for turbulence generation. P_d is calculated using eq 1, where ρ is the air density (1.233 kg m^{-3} at the mean measurement temperature of 12.9 °C and 101.3 kPa), C_d is the drag coefficient (Section 2.2.2), A is the vehicle frontal area, and v is the measured vehicle speed.[24] A benefit of the vehicle technical information is the ability to calculate the frontal area and P_d for individual vehicles from their dimension measurements.

$$TKE \propto P_d = \frac{1}{2}\rho C_d A v^3 \quad (1)$$

For assessing the impact of vehicle-induced turbulence and aerodynamic properties on near-road TRAP, vehicles were grouped by type, fuel type, exhaust position, and losses due to aerodynamic drag, P_d. Drag losses were calculated using eq 1 and expressed in categories as quantiles (Low < 0.25, 0.25 ≤ Low-mid < 0.50, 0.50 ≤ High-mid < 0.75, 0.75 ≤ High), calculated independently for each vehicle type and fuel type subgroup. The calculation of quantiles was necessary as the plume regression method requires defined vehicle groupings.

2.2.4. Emission Rates. The CO_2 coefficients calculated from plume regression reflect the expected near-road concentration increment associated with each vehicle group, and are influenced by both CO_2 emission rate, and subsequent dispersion (related to exhaust position and aerodynamic properties). To isolate the contribution of dispersion and the impact of vehicle design characteristics, two metrics for CO_2 emission rates were used in this study. Neither of the emission

https://doi.org/10.1021/acsestair.5c00059
ACS EST Air 2025, 2, 1089−1098

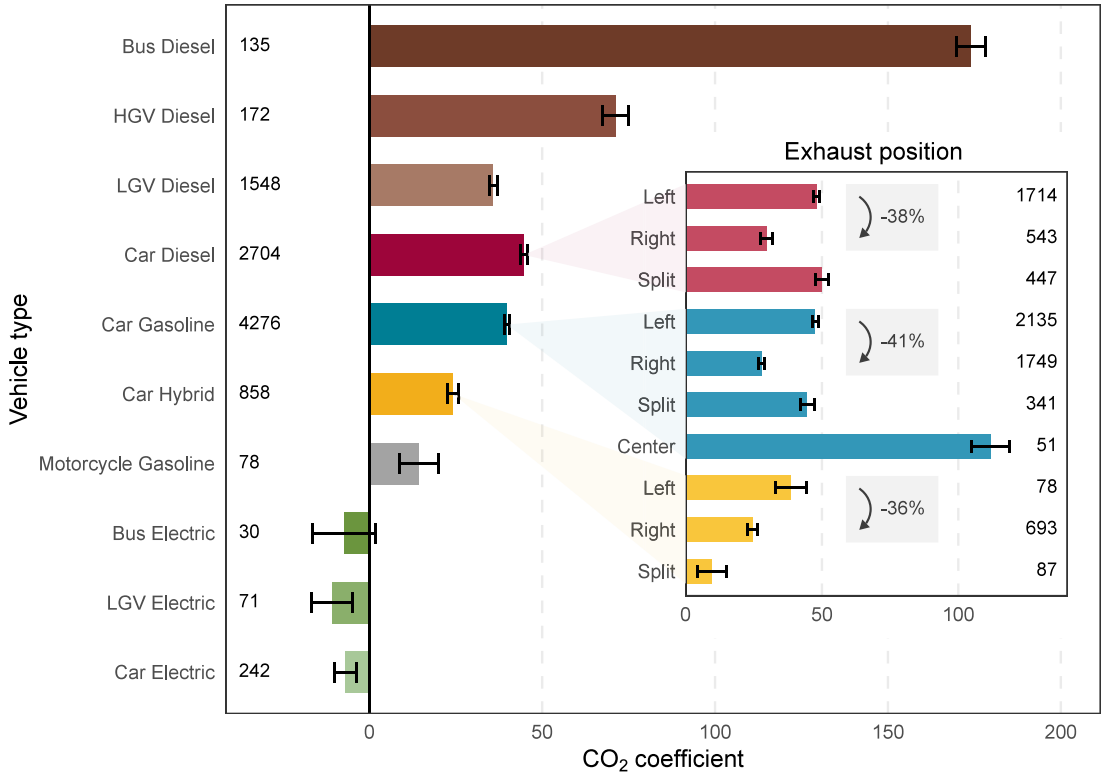

Figure 1. CO_2 coefficients for vehicle type and fuel type groups. The inset plot further separates passenger cars by the exhaust position. Error bars represent 95% confidence intervals, and number labels denote vehicle group sample sizes. Gray boxes display the reduction in CO_2 coefficient for right exhaust positions compared to left for each fuel type. The exhaust locations include those manually assigned and predicted.

rate values can be directly compared to the plume regression coefficients that provide concentration and not emission estimates. However, these emission factors are useful to understand the extent to which roadside concentrations are associated with emissions rather than dispersion influences.

For the exhaust position analysis (Section 3.1), Type-Approval CO_2 emission rates based on laboratory test cycles (g km^{-1}), available from the vehicle technical information, were aggregated to calculate a mean value for each vehicle group. These emission rates are listed in Table S6. The mean Type-Approval CO_2 emission rate reflects an average value across a range of driving conditions and was chosen as it could be calculated for all vehicle types.

For the vehicle-induced turbulence and aerodynamic properties analysis (Section 3.4), which included only cars and LGVs, instantaneous CO_2 emission rates were modeled for individual vehicles. Instantaneous fuel consumption (kg/s) was calculated using the Passenger Car and Heavy Duty Emission Model (PHEM), incorporating vehicle speed, acceleration, road gradient, and technical data (e.g., mass, dimensions, engine specs).[27,28] These rates were then converted into CO_2 emission rates (g s^{-1}) using standard emission factors: 3.16 g kg^{-1} for gasoline and 3.17 g kg^{-1} for diesel.[29] Finally, the values were aggregated for each vehicle group and used to normalize the plume regression CO_2 coefficients. Modeled instantaneous CO_2 emission rates provide a more accurate estimate of actual emission at the time of measurement than type-approval values but could not be calculated for all vehicle types due to missing technical data.

3. RESULTS AND DISCUSSION

3.1. Exhaust Position Effect on CO_2. The CO_2 concentration measurements were grouped by vehicle type, fuel type, and exhaust position (passenger cars only) for plume regression. The resulting calculated CO_2 concentration coefficients are shown in Figure 1, with detailed values provided in Table S7. These coefficients represent the increase in roadside CO_2 concentrations associated with each vehicle group. It is important to note that these coefficients differ from vehicle emission factors, as roadside CO_2 concentrations are influenced by emission rates and factors, such as exhaust proximity to the curb and vehicle design features affecting plume dispersion. These measurements therefore offer direct insight into roadside TRAP emissions and dispersion under real-world conditions.

Figure 1 reveals clear trends driven by vehicle type, fuel type, and exhaust position. Larger vehicles, such as buses and HGVs, exhibit higher CO_2 coefficients due to their higher emission rates. Among passenger cars, gasoline hybrid vehicles are associated with the lowest CO_2 coefficients, reflecting their lower emission rates. Furthermore, left exhaust cars consistently produced higher CO_2 coefficients than right exhaust cars across all fuel types, highlighting the importance of the proximity of exhaust to the curb for near-road TRAP concentrations.

Specifically, CO_2 coefficients were reduced by 38%, 41%, and 36% for diesel, gasoline, and gasoline hybrid cars, respectively, when comparing right exhausts to left exhausts. These differences can confidently be attributed to exhaust location, as the mean vehicle speeds, aerodynamic properties, and type approval CO_2 emission rates (Section 2.2.4 and Table S6) for left and right exhaust vehicles within each fuel type

https://doi.org/10.1021/acsestair.5c00059
ACS EST Air 2025, 2, 1089−1098

were very similar, with less than 5% variation across all comparisons. The only exception was for gasoline hybrid cars, where vehicles with right exhausts had a 37% higher mean type approval CO_2 emission rate than those with left exhausts. This may explain why the difference in the CO_2 coefficients was the smallest for gasoline hybrid cars. However, it is important to note that type approval CO_2 emission rates do not perfectly represent real-world driving conditions and serve only as a guide.[30,31]

To evaluate the machine learning algorithm used to assign exhaust positions for cars with nonvisible exhausts in the images, a plume regression was performed categorizing car exhaust groups into manually assigned and predicted positions. The resulting CO_2 coefficients are shown in Figure S7 and Table S8. For manually assigned cars, the CO_2 coefficients were reduced by 60%, 59%, and 75% for diesel, gasoline, and gasoline hybrid vehicles, respectively, when comparing right to left exhaust positions. In contrast, for predicted exhaust positions, the reductions were 23%, 34%, and 4%, respectively. While left-exhaust CO_2 coefficients were similar between manually assigned and predicted groups across all fuel types, right-exhaust CO_2 coefficients were approximately twice as high for predicted positions compared to manually assigned ones.

A likely explanation for these observations is exhaust *orientation*, which has been shown in the literature to influence plume dispersion and near-road concentrations.[14] Manually assigned exhausts are all horizontal, and predicted exhausts can all be assumed to be down-turned. Horizontal exhausts result in more dispersion and lower roadside concentrations, while down-turned exhausts result in less dispersion and higher roadside concentrations. Even though the predicted exhaust positions are not visible, these results show that there is a consistent left−right difference in the CO_2 coefficient. However, hidden (down-turned) exhausts are associated with different dispersion characteristics compared with horizontal exhausts.

The CO_2 coefficient for gasoline cars with center exhausts in Figure 1 was 1.4 and 3.0 times higher than those for those with left and right exhausts, respectively. This increase is likely due to these vehicles being high-performance models with lower fuel efficiency and higher CO_2 emission rates, as confirmed by technical data showing that all 51 center-exhaust cars were classified as *sport* models with a 17.6% higher mean type-approval CO_2 emission rate. Additionally, center exhausts release exhaust gases directly into the wake zone of the vehicle, where the interaction of turbulence and plume dispersion could result in higher measured CO_2 concentrations when compared to exhaust positioned in other locations.[14] More research with direct turbulence measurements, such as using a sonic anemometer, is needed to better understand these interactions.

For split exhaust cars, CO_2 coefficients were similar to those with right exhausts for diesel and gasoline fuel but much lower than both left and right exhausts for gasoline hybrid fuel. Split exhaust diesel and gasoline cars exhibited mean Type Approval CO_2 emission rates that were 30−34% and 10−13% higher, respectively, compared to left and right exhaust cars. This difference may partially explain the observed results. Another contributing factor is the uneven distribution of exhaust gases in split exhaust systems, a characteristic that varies across manufacturers and models, and could not be further discerned in this work.[32] Additionally, some vehicle manufacturers install fake exhaust outlets to enhance vehicle aesthetics, even when the true exhaust is hidden on the left or right.[33] Where such fake exhausts were obvious, these vehicles were classified as unknown during the exhaust position assignment. However, it is important to note that a small number of vehicles may have been incorrectly classified as split.

Exhaust position also likely explains the differences observed between diesel buses and HGVs. Despite similar Type Approval CO_2 emission rates, the CO_2 concentration coefficient for buses was 2.4 times higher than that for HGVs. Diesel buses typically have exhausts located low at the rear, often visible on the right-hand side in vehicle images, whereas HGV exhausts are more varied in placement, often higher on the vehicle toward the front and not visible in any images. This placement results in greater dispersion of exhaust gases before reaching the PS instruments for HGVs compared to buses, reducing their CO_2 concentration coefficients. Other factors influencing dispersion, such as vehicle speed and aerodynamic properties, were similar among the two vehicle groups.

For diesel LGVs, the CO_2 coefficient is lower than that of diesel cars with left exhausts but higher than those with right exhausts. LGVs have a type approval CO_2 emission rate 38% higher than cars with either left or right exhausts. While exhaust locations for LGVs could not be assigned, the CO_2 coefficient results suggest that most LGVs likely had the right exhausts, based on their relative values when compared to diesel cars. LGVs had a greater mean frontal area but lower mean speed than diesel cars; these factors likely influence roadside exhaust dispersion in opposing ways, though detailed conclusions are limited by the available data.

These findings highlight the significant impact of vehicle design characteristics on near-road CO_2 and TRAP concentrations. Of all cars (excluding EVs), 38% had right-positioned exhausts, associated with the lowest CO_2 coefficients and roadside TRAP concentrations. If the remaining cars repositioned their exhausts to the right, the average CO_2 coefficient for cars—and thus roadside TRAP concentration contributions—could decrease by 29%. Achieving a comparable reduction through improvements in catalyst after-treatment systems would be far more challenging.

While it is unlikely that existing vehicles would be retrofitted with repositioned exhausts due to cost and engineering constraints, exhaust placement could be considered in the design of future vehicles. Although most vehicle models are built on global platforms, regional adaptation—such as steering column layout, headlight beam patterns, and emissions control settings—are already common.[34] In this context, the exhaust position represents a feasible design consideration that could be aligned with local driving practices to reduce near-road TRAP exposure. Given the expected continued production of fossil-fueled (particularly hybrid) vehicles over the coming decades, there remains scope for manufacturers to reduce near-road TRAP concentrations through design choices.[35]

The effect of exhaust position is particularly important for diesel cars in the UK, where only 20% of vehicles had the right exhausts. Repositioning the exhausts of the remaining cars could reduce their roadside TRAP contributions by 33%, which is especially important given the historically higher NO_x and particulate matter (PM) emissions from diesel cars. It is important to note that exhaust repositioning does not reduce the overall TRAP emissions. However, the primary concern with these pollutants is their harmful impacts on human health,

https://doi.org/10.1021/acsestair.5c00059
ACS EST Air 2025, 2, 1089−1098

so minimizing roadside exposure through any means remains a priority.

Passenger car exhaust position often reflects the production region's left- or right-hand traffic practices, with vehicles designed to position exhausts on the offside (furthest from the curb). Of the measured cars, 76% were manufactured in regions that drive on the right-hand side of the road, opposite to the UK, explaining why the minority of vehicles had exhausts positioned on the right — the optimal position to minimize near road TRAP in the UK. Exhaust position is therefore disproportionately important in the UK, where vehicles drive on the left-hand side, but the passenger car fleet predominantly comprises models produced for right-hand driving regions.

The global implications of these results are also important. In all regions, the international vehicle market ensures that a portion of the fleet will have exhausts positioned closest to the curb, regardless of left- or right-hand driving practices. Insights into the impacts of exhaust position on near-road TRAP concentrations from this study demonstrate the value of combining fast-response roadside measurements with individual vehicle data. The current work also shows the importance of vehicle design factors in helping to explain near-road concentrations of TRAP. Future research should prioritize quantifying how exhaust position effects diminish with increasing lateral and vertical distances from the road. One approach to achieve this is through controlled release experiments, where a tracer gas is emitted from various points on a vehicle to simulate different exhaust positions.

3.2. Exhaust Position Effect on NO_x. To more directly assess the impact of the exhaust position on roadside TRAP concentrations, plume regression was performed for NO_x using the same vehicle groups analyzed for CO_2. The NO_x concentration coefficient values for each group are presented in Figure S8 and Table S9. Unlike CO_2, NO_x emission rates vary significantly based on fuel type and after-treatment systems, adding complexity to vehicle group comparisons. For this reason, CO_2 was the primary focus of this analysis. However, the NO_x results provide valuable insight into near-road TRAP.

Diesel cars had NO_x concentration coefficients 5.2 and 6.5 times higher than those of gasoline cars for left and right exhaust positions, respectively, highlighting their significantly greater contribution to near-road NO_x concentrations, consistent with reported emission rates.[36,37] For right exhaust cars, NO_x coefficients were 27.9%, 75.9%, and 34.0% lower than for left exhaust cars for diesel, gasoline, and gasoline hybrid vehicles, respectively, in agreement with the CO_2 findings (Section 3.1). The greater variability compared to that of CO_2 likely reflects the higher signal-to-noise ratio in the NO_x increment data, especially for lower NO_x emitting gasoline and gasoline hybrid vehicles.

NO_x/CO_2 ratios (ppb ppm^{-1}) were calculated from the plume regression data sets to ensure differences in NO_x coefficients between left and right exhaust cars were due to exhaust position, rather than differences in NO_x emission rates due to variations in variables such as vehicle manufacturer, body type, or engine size. These ratios isolate NO_x emission rates by removing the influence of exhaust location and dispersion, assuming a similar dispersion for CO_2 and NO_x.

Vehicle emission remote sensing is another roadside measurement technique that uses cross-road spectroscopy to capture emissions from the entire vehicle plume. Emission ratios obtained from PS have previously shown to agree well with those from remote sensing.[13] A representative sample of remote sensing measurements, collected in 2022, was selected to match the PS data in terms of sample size, fuel type distribution, and Euro class distribution. The random forest machine learning algorithm (trained and used on the PS data) was applied to this remote sensing sample to assign exhaust positions to vehicle measurements. The NO_x/CO_2 ratios from the remote sensing sample were then aggregated by the fuel type and exhaust position, as shown in Table 1.

Table 1. NO_x/CO_2 Ratios for Cars Grouped by Fuel Type and Exhaust Location, Derived from Point Sampling and a Representative Sample of Remote Sensing Data[a]

		NO_x/CO_2 (ppm ppb^{-1})	
Fuel Type	Exhaust Position	Point Sampling	Remote Sensing
Diesel	Left	2.74 ± 0.07	2.85 ± 0.17
Diesel	Right	3.18 ± 0.25	3.41 ± 0.35
Gasoline	Left	0.54 ± 0.03	0.46 ± 0.09
Gasoline	Right	0.52 ± 0.06	0.39 ± 0.08
Hybrid	Left	0.17 ± 0.20	0.59 ± 0.34
Hybrid	Right	0.20 ± 0.11	0.32 ± 0.08

[a]Hybrid refers to gasoline hybrid vehicles. The uncertainty values represent 95% confidence intervals.

The NO_x/CO_2 ratios derived from PS and the remote sensing sample align with values reported in the literature.[36] Strong agreement (all values within 95% confidence intervals) between the two data sets, summarized in Table 1, supports plume regression as a highly robust technique for assessing roadside vehicle emissions. Additionally, the similar NO_x/CO_2 ratio values for left and right exhaust vehicles indicate that the observed differences in NO_x coefficients are primarily due to the exhaust position. Repositioning the exhausts of all cars to the right-hand side would reduce the average NO_x coefficient, and therefore average contribution of cars toward roadside NO_x increment concentrations by 26.1%, directly demonstrating the impact of vehicle design choices on near-road TRAP concentrations.

For NO_2, patterns similar to those observed for total NO_x were found across vehicle types and exhaust locations, with NO_2 concentration coefficients presented in Table S9. The trends in NO_2 concentration coefficients mirrored those of NO_x, but were approximately five times smaller in magnitude. In the case of NO_2 concentrations there are two principal contributions to curbside concentrations: the directly emitted (primary) NO_2 from vehicles and the contribution from NO reacting with ozone (O_3) to produce secondary NO_2. At other sites and for other conditions e.g. warm, sunny weather where secondary NO_2 formation could be enhanced, there could be differences in the behavior of NO_2 and total NO_x, which would warrant further investigation.

A promising future extension of this work is the fast-response measurement of additional pollutants. PS has proven effective for measuring vehicular PM, a pollutant of significant concern for human exposure and health.[12] Combining fast-response PM measurements with the plume regression approach could offer new insights into how exhaust position and roadside dispersion processes influence near-road PM mass and particle number (PN) concentrations.

https://doi.org/10.1021/acsestair.5c00059
ACS EST Air 2025, 2, 1089−1098

3.3. Electric Vehicles. Plume regression produced *negative* CO_2 concentration coefficients for EVs (Figure 1), indicating that the passing of these vehicles is associated with a *decrease* in near-road CO_2 and TRAP concentrations. This finding was reinforced by a negative average plume profile for isolated EV measurements, as shown in Figure S9. A likely explanation of this observation is that EVs disperse the plumes of nearby fossil-fueled vehicles through vehicle-induced turbulence, which is influenced by the EV's aerodynamic properties (frontal area and drag coefficient), speed, and existing traffic TRAP concentrations due to fossil-fueled vehicles.

Aerodynamic properties primarily depend on the frontal area, which directly influences induced turbulence (eq 1). Larger, less aerodynamic EVs should therefore produce more turbulence and dispersion. Thus, electric buses are expected to have the most negative CO_2 coefficients, followed by electric LGVs and electric cars, given their relative sizes. However, the CO_2 coefficients for EVs are also strongly influenced by vehicle speed (which has a cubic relationship to induced turbulence) and existing exhaust gas concentrations, both of which are dependent on traffic flow and measurement location.

PS measurements were made at three sites: low-traffic sites A and B, with average vehicle gaps of 15.5 s and speeds of 34.5 km h^{-1}, and high-traffic site C, with a 7.0 s gap and 44.2 km h^{-1} average speed. All electric buses, 80% of electric LGVs, and 34% of electric cars were measured at low-traffic locations, with the remainder sampled at the high-traffic site. Detailed driving conditions for each site are listed in Table S1. The low CO_2 coefficient for electric buses is likely due to their slower speeds and lower CO_2 concentrations at low-traffic sites A and B, with an average speed of 32.3 km h^{-1} and a vehicle gap of 18.2 s. Although more electric LGVs were measured at low-traffic locations compared to electric cars, their more negative CO_2 coefficient suggests that the differences in the frontal area and the resulting impact on turbulence dominate the results.

To further investigate EV impacts on near-road TRAP concentrations, the electric car group was divided by measurement location into low-traffic (sites A and B) and high-traffic (site C) categories, and the plume regression was rerun for CO_2. The updated CO_2 coefficients for EVs are presented in Figure 2, while the coefficients for non-EVs remained unchanged. The CO_2 coefficients, average speeds, frontal areas, and drag coefficients of the EV subgroups used in the revised plume regression are summarized in Table S10.

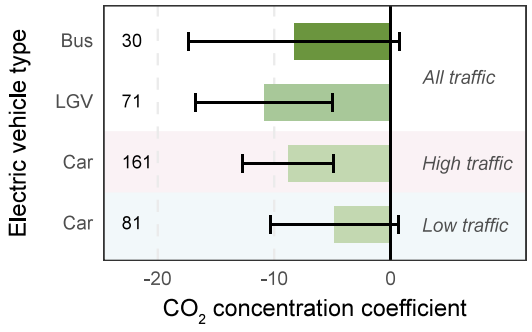

Figure 2. CO_2 concentration coefficients for the EVs. Electric cars are disaggregated into those measured at the high- and low-traffic sites. The error bars represent 95% confidence intervals and the text labels denote traffic condition.

The CO_2 concentration coefficient for electric cars at the high-traffic site was 83% more negative than that at low-traffic sites, despite comparable frontal areas and drag coefficients. This difference is attributed to a 29% greater mean speed at the high-traffic site, which would act to enhance the dilution of exhaust plumes from other nearby vehicles. Indeed, the higher speed alone may account for the observed CO_2 coefficient decrease, as vehicle-induced turbulence is proportional to the cube of speed ($1.29^3 = 2.15$, 115% increase in turbulence from speed). However, it is likely that existing concentrations of CO_2 at the high-traffic site were also greater, given the driving conditions and smaller average vehicle gap. The large 95% confidence intervals, due to relatively small sample sizes, highlight the need for further research to better isolate these variables.

It is also important to consider differences in site characteristics that may influence the calculated CO_2 concentration coefficients such as variations in geometry and local topography at each measurement location. These factors are explored in more detail in the individual site analyses presented in the Supporting Information (Figures S4 and S5, Table S2). At Site B (low-traffic), the CO_2 concentration coefficient for electric cars was four times more negative than that at Sites A (low-traffic) and C (high-traffic). Consequently, the CO_2 concentration coefficient for cars at low-traffic sites in Figure 2 is likely more negative than that expected under more uniform measurement conditions. This suggests that the true difference between high- and low-traffic sites may be greater than reported.

3.4. Aerodynamic Properties. To further investigate the role of vehicle-induced turbulence, we considered the relationship between the CO_2 coefficient and P_d. For cars and LGVs, plume regression was run on four P_d quantile groups (Section 2.2.3). Cars were separated into fossil-fueled and electric groups, and the resulting CO_2 concentration coefficients are shown in panels A and B of Figure 3. Exact coefficient values and additional information are listed in Table S11.

For fossil-fueled cars, the relationship between vehicle-induced turbulence (P_d quantile) and measured CO_2 concentrations is complex. As P_d increases, both dispersion and CO_2 emission rates rise due to the impact of P_d on the engine load, which influences fuel consumption and emissions. Panel A of Figure 3 shows the CO_2 concentration coefficients for fossil-fueled cars, reflecting the combined effect of the emission rate and the near-road dispersion. Exhaust position distributions were similar across all four quantiles.

Panel C isolates the emission rate component of this relationship, presenting mean instantaneously modeled CO_2 emission rates for each P_d quantile (Section 2.2.4). With increasing P_d quantile (Low to High), the increasing drag force means that the vehicle's engine load is higher, thus fuel consumption and CO_2 emission rate also increase.

To isolate the effect of vehicle-induced turbulence, the CO_2 concentration coefficients in panel A were normalized by the emission rates in Panel B, using the Low P_d quantile emission rate as the baseline (1.0). While the normalized CO_2 concentration coefficients, shown in panel E, do not show a perfect decrease with increasing P_d, normalization does shift the results toward expectation, eliminating the initial increase from Low to Low-mid P_d (likely due to rising CO_2 emissions) and revealing a clear downward trend from High-mid to High P_d. Similar findings for LGVs are presented in Figure S10.

https://doi.org/10.1021/acsestair.5c00059
ACS EST Air 2025, 2, 1089−1098

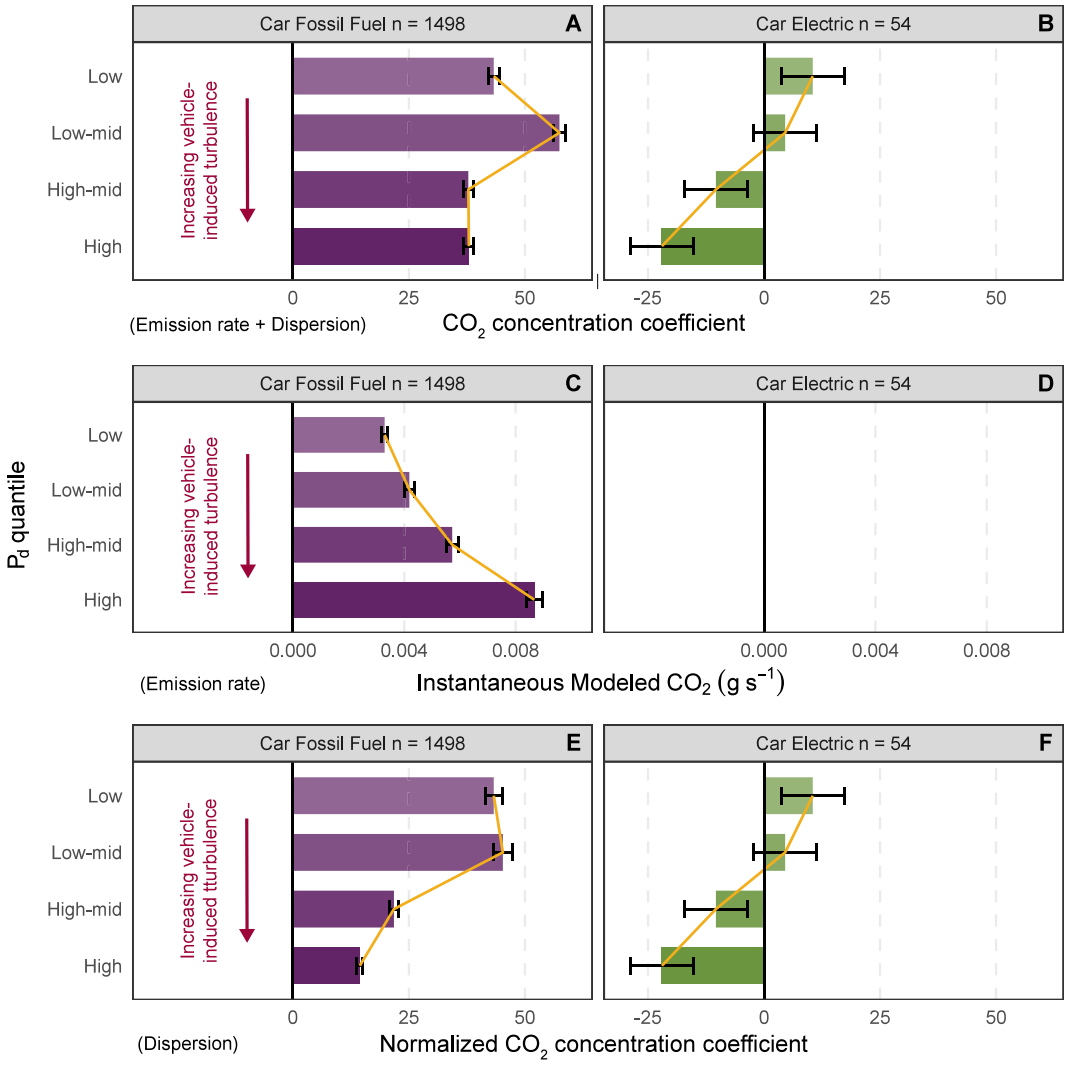

Figure 3. CO_2 concentration coefficient (A and B), instantaneous modeled CO_2 (C and D), and CO_2 concentration coefficient normalized by instantaneous modeled CO_2 (E and F) for fossil-fueled and electric passenger cars, grouped by P_d quantile. The error bars represent 95% confidence intervals, and the yellow lines show the trends across quantiles.

Because electric cars do not emit CO_2, they serve as an ideal baseline for evaluating the effects of vehicle-induced turbulence on near-road TRAP concentrations. From P_d quantile Low to High, the electric car CO_2 coefficient becomes increasingly negative, highlighting the role of EV-induced turbulence in dispersing CO_2 and reinforcing the findings in the previous section. Over this range, the mean vehicle speed increased by 75%, while the frontal area increased by 2.8%. Because speed and frontal area are the primary drivers of turbulence, the stronger correlation with speed suggests that it is the dominant factor behind the increasingly negative CO_2 coefficients.

Positive CO_2 coefficients for electric cars in lower P_d quantiles can be attributed to two factors. First, low turbulence in these quantiles may not effectively disperse CO_2 from other traffic, leading the plume regression to attribute residual CO_2 to electric cars. Second, low P_d electric cars represent the smallest CO_2 concentration increments; therefore, minor deviations from local background concentrations have a larger impact on coefficient variability.

Emission rates were not calculated for electric cars; therefore, no normalization was applied, making panels F and A identical. If the modeled CO_2 emission rates for fossil-fueled cars perfectly captured the true emissions during vehicle measurements, the normalized CO_2 coefficients in panel E would isolate the dispersion effects on roadside CO_2 concentrations and closely match the trend observed for electric cars in panel F. However, modeling inaccuracies and variability in the PS data introduce discrepancies, and additional research is required to draw further conclusions.

These findings demonstrate that vehicle-induced turbulence directly affects roadside CO_2 and TRAP concentrations, with the impact increasing with P_d. While aerodynamic properties such as frontal area and drag coefficient contribute, vehicle speed plays a more significant role due to its greater variation and cubed relationship with P_d. For fossil-fueled vehicles, turbulence and dispersion effects on roadside CO_2 and TRAP concentrations are closely linked to emission rates, which also rise with increasing P_d.

In addition to the findings for exhaust position (Sections 3.1 and 3.2), these results have important implications for the thousands of near-road ambient air quality sites worldwide as well as for air quality simulation models in near-road and street canyon environments. This work suggest that aerodynamic properties and exhaust position may introduce systematic

https://doi.org/10.1021/acsestair.5c00059
ACS EST Air 2025, 2, 1089−1098

biases in measured or predicted pollutant concentrations. Considering these physical vehicle attributes in roadside monitoring analyses and dispersion modeling is therefore likely to enhance accuracy. Future research in this area should explore the interaction between vehicle-induced turbulence and roadside TRAP concentrations using sonic anemometers to provide a direct measure of TKE. This work could be extended by considering how the measured effect vary with near-road geometry and meteorological conditions.

■ ASSOCIATED CONTENT

Supporting Information

The Supporting Information is available free of charge at https://pubs.acs.org/doi/10.1021/acsestair.5c00059.

Photos of PS measurement sites A, B and C; three different plume profiles tested in the plume regression approach; scatter plot showing the relationship between calculated CO_2 coefficients; plume profiles for each measurement site; passenger car CO_2 coefficients for fuel type, exhaust position, and measurement site groups; example images of the different manually assigned exhaust positions; CO_2 coefficients for passenger cars with left and right exhaust positions, split into manually assigned and predicted groups; NO_x coefficients for vehicle type, fuel type, and exhaust position groups; plume profile for electric vehicles; CO_2 concentration coefficients and aerodynamic properties; driving conditions and vehicle fleet composition (vehicle type, fuel type, and emission standard); passenger car CO_2 concentration coefficients for fuel type, exhaust position, and site groups; passenger car exhaust position random forest prediction model training parameters and performance metrics; summary of the manually assigned and predicted passenger car exhaust positions; dimension classifications and aerodynamic drag coefficients; mean type approval CO_2 emission rates for vehicle type, fuel type, and exhaust position groups; CO_2 concentration coefficients for vehicle type, fuel type, and exhaust position groups; passenger car CO_2 concentration coefficients for fuel type, exhaust position, and exhaust assignment source groups; NO_x and NO_2 concentration coefficients and standard errors (SE); CO_2 coefficient, mean speed, mean frontal area, and mean drag coefficient for electric vehicles; CO_2 concentration coefficient, mean power of drag P_d, mean vehicle speed V, mean frontal area A, and mean drag coefficient C_d (PDF)

■ AUTHOR INFORMATION

Corresponding Author

David C. Carslaw − *Wolfson Atmospheric Chemistry Laboratories, University of York, York YO10 5DD, United Kingdom;* orcid.org/0000-0003-0991-950X; Email: david.carslaw@york.ac.uk

Authors

Samuel Wilson − *Wolfson Atmospheric Chemistry Laboratories, University of York, York YO10 5DD, United Kingdom*

Naomi J. Farren − *Wolfson Atmospheric Chemistry Laboratories, University of York, York YO10 5DD, United Kingdom;* orcid.org/0000-0002-5668-1648

Yoann Bernard − *The International Council on Clean Transportation, 10623 Berlin, Germany*

Marvin D. Shaw − *Wolfson Atmospheric Chemistry Laboratories, University of York, York YO10 5DD, United Kingdom; National Centre for Atmospheric Science, University of York, York YO10 5DD, United Kingdom;* orcid.org/0000-0001-9954-243X

Kaylin Lee − *The International Council on Clean Transportation, 10623 Berlin, Germany*

Mallery Crowe − *The International Council on Clean Transportation, 10623 Berlin, Germany*

James D. Lee − *Wolfson Atmospheric Chemistry Laboratories, University of York, York YO10 5DD, United Kingdom; National Centre for Atmospheric Science, University of York, York YO10 5DD, United Kingdom*

Complete contact information is available at: https://pubs.acs.org/10.1021/acsestair.5c00059

Notes

The authors declare no competing financial interest.

■ ACKNOWLEDGMENTS

We express our gratitude to The Real Urban Emissions Initiative for funding this work. The authors also acknowledge the financial support from Ricardo and the Department of Chemistry at the University of York for Sam Wilson's PhD studentship. We thank Airyx GmbH for their technical support with the ICAD analyzer, and our thanks extend to Will Drysdale, Martyn Ward, Stuart Young, Sam Rogers and Katie Read at the University of York for their support with instrument operation.

■ ABBREVIATIONS

ALPR - Automatic License Plate Recognition
ANPR - Automatic Number Plate Recognition
CO_2 - Carbon Dioxide
DVLA - Driver and Vehicle Licensing Agency
EV - Electric Vehicle
HGV - Heavy Goods Vehicle
LGV - Light Goods Vehicle
NO - Nitrogen Oxide
NO_2 - Nitrogen Dioxide
NO_x - Nitrogen Oxides
PHEM - Passenger Car and Heavy Duty Emission Model
PS - Point Sampling
SMMT - Society of Motor Manufacturers and Traders
TKE - Turbulent Kinetic Energy
TRAP - Traffic Related Air Pollution

■ REFERENCES

(1) Anenberg, S.; Miller, J.; Henze, D.; Minjares, R. *A global snapshot of the air pollution-related health impacts of transportation sector emissions in 2010 and 2015*; International Council on Clean Transportation: Washington, DC, 2019; pp 1−48.

(2) HEI Traffic-Related Air Pollution: a Critical Review of the Literature on Emissions, Exposure, and Health Effects. Health Effects Institute. Panel on the Health Effects of Traffic-Related Air Pollution.2010; https://www.healtheffects.org/system/files/SR17TrafficReview.pdf, Date accessed: 2024−12−19.

(3) Bell, J.; Honour, S. L.; Power, S. A. Effects of vehicle exhaust emissions on urban wild plant species. *Environ. Pollut.* **2011**, *159*, 1984−1990.

(4) Xie, P.; Zhang, C.; Wei, Y.; Zhu, R.; Chu, Y.; Chen, C.; Wu, Z.; Hu, J. Status of near-road air quality monitoring stations and data application. *Atmospheric Environment: X* **2024**, *23*, 100292.
(5) Apte, J. S.; Messier, K. P.; Gani, S.; Brauer, M.; Kirchstetter, T. W.; Lunden, M. M.; Marshall, J. D.; Portier, C. J.; Vermeulen, R. C. H.; Hamburg, S. P. High-Resolution Air Pollution Mapping with Google Street View Cars: Exploiting Big Data. *Environ. Sci. Technol.* **2017**, *51*, 6999−7008.
(6) Wilde, S. E.; Padilla, L. E.; Farren, N. J.; Alvarez, R. A.; Wilson, S.; Lee, J. D.; Wagner, R. L.; Slater, G.; Peters, D.; Carslaw, D. C. Mobile monitoring reveals congestion penalty for vehicle emissions in London. *Atmospheric Environment: X* **2024**, *21*, 100241.
(7) Wilson, S.; Farren, N. J.; Wilde, S. E.; Wagner, R. L.; Lee, J. D.; Padilla, L. E.; Slater, G.; Peters, D.; Carslaw, D. C. Mobile monitoring reveals the importance of non-vehicular particulate matter sources in London. *Environmental Science: Processes & Impacts* **2024**, *26*, 2145−2157.
(8) Brimblecombe, P.; Chu, M.; Liu, C.-H.; Fu, Y.; Wei, P.; Ning, Z. Roadside NO2/NOx and primary NO2 from individual vehicles. *Atmos. Environ.* **2023**, *295*, 119562.
(9) Chu, M.; Brimblecombe, P.; Gali, N. K.; Ghadikolaei, M. A.; Wei, P.; Li, X.; Yang, S.; Wei, Y.; Ning, Z. Roadside measurement of N_2O and CH_4 emissions from vehicles in Hong Kong. *Science of The Total Environment* **2024**, *956*, 177241.
(10) Preble, C. V.; Dallmann, T. R.; Kreisberg, N. M.; Hering, S. V.; Harley, R. A.; Kirchstetter, T. W. Effects of Particle Filters and Selective Catalytic Reduction on Heavy-Duty Diesel Drayage Truck Emissions at the Port of Oakland. *Environ. Sci. Technol.* **2015**, *49*, 8864−8871.
(11) Khreis, H.; Warsow, K. M.; Verlinghieri, E.; Guzman, A.; Pellecuer, L.; Ferreira, A.; Jones, I.; Heinen, E.; Rojas-Rueda, D.; Mueller, N.; et al. The health impacts of traffic-related exposures in urban areas: Understanding real effects, underlying driving forces and co-producing future directions. *Journal of Transport & Health* **2016**, *3*, 249−267.
(12) Knoll, M.; Penz, M.; Juchem, H.; Schmidt, C.; Pöhler, D.; Bergmann, A. Large-scale automated emission measurement of individual vehicles with point sampling. *Atmospheric Measurement Techniques* **2024**, *17*, 2481−2505.
(13) Farren, N. J.; Wilson, S.; Bernard, Y.; Shaw, M. D.; Lee, K.; Crowe, M.; Carslaw, D. C. An ambient measurement technique for vehicle emission quantification and concentration source apportionment. *Environ. Sci. Technol.* **2024**, *58*, 20091.
(14) Plogmann, J.; Stauffer, C.; Dimopoulos Eggenschwiler, P.; Jenny, P. URANS Simulations of Vehicle Exhaust Plumes with Insight on Remote Emission Sensing. *Atmosphere* **2023**, *14*, 558.
(15) Xiang, S.; Zhang, S.; Brimblecombe, P.; Yu, Y. T.; Noll, K. E.; Liu, H.; Wu, Y.; Hao, K. An Integrated Field Study of Turbulence and Dispersion Variations in Road Microenvironments. *Environ. Sci. Technol.* **2024**, *58*, 20566−20576.
(16) Airyx ICAD In Situ NO_x Monitor, 2023; https://airyx.de/item/icad/, Date accessed: 2024−10−17.
(17) Horbanski, M.; Pöhler, D.; Lampel, J.; Platt, U. The ICAD (iterative cavity-enhanced DOAS) method. *Atmospheric Measurement Techniques* **2019**, *12*, 3365−3381.
(18) Rekor OpenALPR Rekor CarCheck Vehicle Recognition API, 2023; https://www.openalpr.com/software/carcheck, Date accessed: 2023−12−10.
(19) Padilla, L. E.; Ma, G. Q.; Peters, D.; Dupuy-Todd, M.; Forsyth, E.; Stidworthy, A.; Mills, J.; Bell, S.; Hayward, I.; Coppin, G.; Moore, K.; Fonseca, E.; Popoola, O. A.; Douglas, F.; Slater, G.; Tuxen-Bettman, K.; Carruthers, D.; Martin, N. A.; Jones, R. L.; Alvarez, R. A. New methods to derive street-scale spatial patterns of air pollution from mobile monitoring. *Atmos. Environ.* **2022**, *270*, 118851.
(20) Venables, W. N.; Ripley, B. D. *Modern Applied Statistics with S*, 4th ed.; Springer: New York, 2002; ISBN 0−387−95457−0.
(21) Breiman, L.; Cutler, A. *randomForest: Breiman and Cutlers Random Forests for Classification and Regression*; 2024; https://CRAN.R-project.org/package=randomForest, Accessed: 2024−06−20.
(22) Kuhn, M. *caret: Classification and Regression Training*; 2023; https://CRAN.R-project.org/package=caret, Accessed: 2024−06−20.
(23) Kühlwein, J. *Driving resistances of light-duty vehicles in Europe: present situation, trends, and scenarios for 2025*. 2016; https://theicct.org/sites/default/files/publications/ICCT_LDV-Driving-Resistances-EU_121516.pdf, Date accessed: 2025−05−12.
(24) Schuetz, T. C. *Aerodynamics of road vehicles*; SAE International, 2015; ISBN: 978−0-7680−7977−7.
(25) Vachon, G.; Louka, P.; Rosant, J.; Mestayer, P.; Sini, J. Measurements of traffic-induced turbulence within a street canyon during the Nantes' 99 experiment. *Water, Air and Soil Pollution: Focus* **2002**, *2*, 127−140.
(26) Thaker, P.; Gokhale, S. The impact of traffic-flow patterns on air quality in urban street canyons. *Environmental pollution* **2016**, *208*, 161−169.
(27) Hausberger, S. *Simulation of Real World Vehicle Exhaust Emission*; Technische Universität Graz, 2003; Vol. *82*; ISBN: 3−901351−74−4.
(28) Davison, J.; Bernard, Y.; Borken-Kleefeld, J.; Farren, N. J.; Hausberger, S.; Sjödin, Å; Tate, J. E.; Vaughan, A. R.; Carslaw, D. C. Distance-based emission factors from vehicle emission remote sensing measurements. *Sci. Total Environ.* **2020**, *739*, 139688.
(29) Bernard, Y.; Tietge, U.; German, J.; Muncrief, R. *Determination of real world emissions from passenger vehicles using remote sensing data*; 2018; https://theicct.org/wp-content/uploads/2021/06/TRUE_Remote_sensing_data_20180606.pdf, Date accessed: 2025−5-12.
(30) Mock, P.; German, J.; Bandivadekar, A.; Riemersma, I. *Discrepancies between type-approval and "real-world" fuel-consumption and CO_2*; 2012; https://theicct.org/wp-content/uploads/2021/06/ICCT_EU_fuelconsumption2_workingpaper_2012.pdf, Date accessed: 2025−05−12.
(31) Fontaras, G.; Zacharof, N.-G.; Ciuffo, B. Fuel consumption and CO_2 emissions from passenger cars in Europe−Laboratory versus real-world emissions. *Progress in energy and combustion Science* **2017**, *60*, 97−131.
(32) MOT MOT inspection manual: cars and passenger vehicles, 8.2 Exhaust emissions.2024; https://www.gov.uk/guidance/mot-inspection-manual-for-private-passenger-and-light-commercial-vehicles/8-nuisance, Date accessed: 2025−05−12.
(33) Exhaust molded trim, part no. 80A807834ET94 Audi Genuine Parts and Accessories.2024; https://parts.audiusa.com/p/Audi_/Trim-molding/131887603/80A807834ET94.html, Accessed: 2025−01−28.
(34) Ravi, S. S.; Osipov, S.; Turner, J. W. Impact of modern vehicular technologies and emission regulations on improving global air quality. *Atmosphere* **2023**, *14*, 1164.
(35) Conway, G.; Joshi, A.; Leach, F.; García, A.; Senecal, P. K. A review of current and future powertrain technologies and trends in 2020. *Transportation Engineering* **2021**, *5*, 100080.
(36) Carslaw, D. C.; Beevers, S. D.; Tate, J. E.; Westmoreland, E. J.; Williams, M. L. Recent evidence concerning higher NOx emissions from passenger cars and light duty vehicles. *Atmos. Environ.* **2011**, *45*, 7053−7063.
(37) Wilson, S.; Farren, N. J.; Rose, R. A.; Wilde, S. E.; Davison, J.; Wareham, J. V.; Lee, J. D.; Carslaw, D. C. The impact on passenger car emissions associated with the promotion and demise of diesel fuel. *Environ. Int.* **2023**, *182*, 108330.

https://doi.org/10.1021/acsestair.5c00059
ACS EST Air 2025, 2, 1089−1098